Density-Functional-Theory-Based Study of Monolayer MoS_2 on Oxide

Amithraj Valsaraj, Leonard F. Register and Sanjay K. Banerjee
Microelectronics Research Center and
Department of Electrical and Computer Engineering
The University of Texas at Austin,
10100 Burnet Road, Bldg. 160, Austin, TX-78758, U.S.A
amithrajv@utexas.edu

Jiwon Chang
SEMATECH
257 Fuller Rd #2200, Albany, NY-12203, U.S.A

Abstract—**Monolayer transition metal dichalcogenides (TMDs) are novel gapped two-dimensional materials with unique electrical and optical properties. Here, we study the effect of dielectric oxide slabs on the electronic structure of monolayer MoS_2 using density functional theory (DFT) calculations. We also have simulated the effects of O-vacancies in the first few layers of the oxide on the band structure of the MoS_2-oxide system, showing here results for vacancies in topmost/MoS_2-adjacent O layer.**

Keywords-component; transition metal dichalcogenides, oxygen vacancies, band structure, atom-projected density of states

I. INTRODUCTION

Monolayer transition metal dichalcogenides (TMDs) are novel materials with unique electrical and optical properties [1]. The two dimensional (2D) nature of monolayer TMDs makes their properties susceptible to the surrounding environment, as evidenced by the mobility enhancement of monolayer MoS_2 when superposed on high-k dielectric such as HfO_2 [2].

Here, we study the effect of HfO_2 and Al_2O_3 on the electronic structure of monolayer MoS_2 using density functional theory (DFT). Two possible terminations for the HfO_2 (Al_2O_3) slab were considered: O-terminated HfO_2 (Al_2O_3) slab with H passivation and Hf (Al) terminated HfO_2 (Al_2O_3) slab. We calculate the band structure and the atom-projected density of states (AP-DOS) for these systems, and compare them to the results for freestanding monolayer MoS_2. We also have simulated the effects of O-vacancies in the first few layers of oxide on the band structure of the MoS_2-oxide system, showing here results for vacancies in the topmost/MoS_2-adjacent O layer.

II. COMPUTATIONAL APPROACH

The DFT calculations were performed using the projector-augmented wave method with a plane-wave basis set as implemented in the Vienna *ab initio* simulation package (VASP). The local density approximation (LDA) was employed for the exchange-correlation potential [3] and the calculated lattice constant is a good match to the experimental value [4]. In our study, two representative dielectrics HfO_2 (chosen for its high-k value) and Al_2O_3 (minimal lattice mismatch) were considered. The hexagonal MoS_2 monolayer was taken to be unstrained, with a volume-relaxed lattice constant of a = 3.122 Å. For the dielectric oxide, the energetically stable crystalline phases of bulk HfO_2 and Al_2O_3 at ambient conditions, namely, monoclinic HfO_2 [5] and hexagonal Al_2O_3 [6], respectively, were utilized.

Our simulations were performed by constructing a supercell of monolayer MoS_2 on an approximately 2 nm thick oxide slabs. For HfO_2, atomic relaxation was performed within a rectangular supercell (a = 9.366 Å, b = 5.407 Å) chosen to reduce the lattice mismatch between monolayer MoS_2 and monoclinic HfO_2, although a roughly 6% strain remains along the in-plane directions in the HfO_2 (Fig. 1). For Al_2O_3, atomic relaxation was performed in a (rotated) hexagonal supercell (a = 8.260 Å) with a strain of only about 0.2%. The systems were relaxed until the Hellmann-Feynman forces on the atoms were less than 0.02 eV/Å. Oxygen vacancies were modeled by removing a single O atom from an O-layer of the supercell.

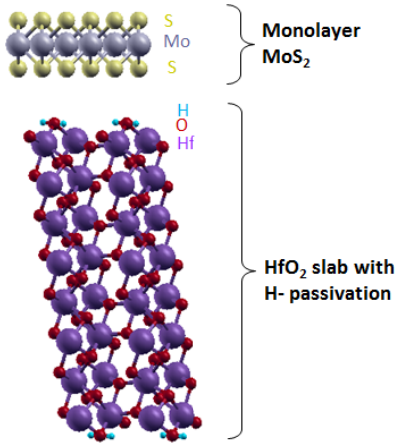

Figure 1. Supercell of monolayer MoS_2 on an H-passivated, O-terminated HfO_2 slab of approximately 2 nm thickness (side view).

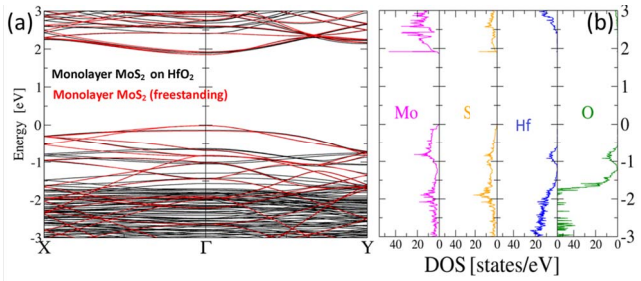

Figure 2. (a) Band structure of monolayer MoS_2 on an O-terminated HfO_2 slab with H-passivation, plotted along the high symmetry directions of the Brillouin zone (black lines). The band structure of freestanding monolayer MoS_2 is superimposed for comparison (red lines). (b) Atom-projected density of states (AP-DOS) for the monolayer MoS_2 and O-terminated HfO_2 system.

III. RESULTS

We have calculated band structure and the atom-projected density of states (AP-DOS) for these systems, and compared the results for the ideal MoS_2-oxide systems to those for freestanding monolayer MoS_2, and the results for the systems with O vacancies to the ideal MoS_2-oxide results.

The simulated band structure of monolayer MoS_2 on O-terminated HfO_2 with H-passivation is shown in Fig. 2(a). In these 0 K simulations, the 0 eV reference corresponds to the highest occupied state. Because a rectangular supercell was used in these simulations, the monolayer MoS_2 band edges at the K point of the freestanding MoS_2 Brillouin zone (BZ) are folded into the Γ point of the supercell's BZ. The band structure of monolayer MoS_2 is largely unaffected by the H-passivated, O-terminated HfO_2. The band gap is devoid of any defect states, suggesting the potential for HfO_2 to act as an excellent insulator or substrate. In addition, the direct band gap is preserved, which is crucial for optoelectronic applications. The absence of band gap states is also evident in the AP-DOS for the system (Fig. 2(b)). In contrast, our results indicate a significant reduction in the band gap of the Hf-terminated HfO_2 slab-MoS_2 system (energy gap E_g of approximately 0.9 eV) as compared to that of freestanding monolayer MoS_2, although a direct band gap is preserved (Fig. 3(a)). We note however, that the valence bands near the Γ point are pulled upward in comparison to freestanding monolayer MoS_2 due to interface defect states arising from the contribution of Hf and O atoms, as illustrated by the non-zero density of states for these atoms near 0 eV in Fig. 3(b).

When an O vacancy is introduced into the top layer of the

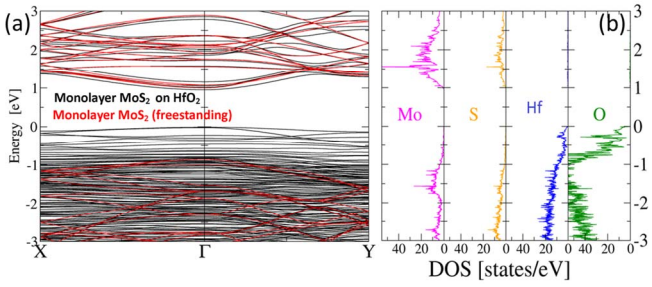

Figure 3. (a) Band structure of monolayer MoS_2 on Hf-terminated HfO_2 slab, plotted along the high symmetry directions of the Brillouin zone (black lines). The band structure of freestanding monolayer MoS_2 is superimposed for comparison (red lines). (b) Atom -projected density of states for the monolayer MoS_2 and Hf-terminated HfO_2 system.

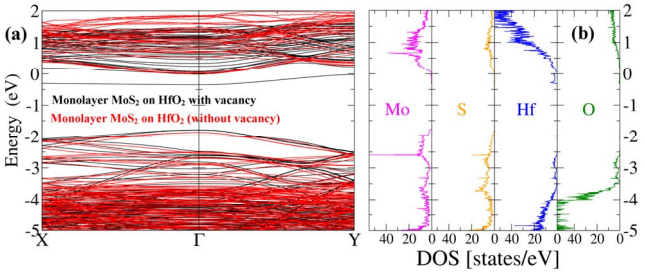

Figure 4. (a) Band structure of monolayer MoS_2 on an H-passivated, O-terminated HfO_2 slab with an O-vacancy in the top layer, plotted along the high symmetry directions of the Brillouin zone (black lines). The band structure of vacancy free monolayer MoS_2-HfO_2 system is superimposed for comparison (red lines). (b) Atom-projected density of states for the monolayer MoS_2 and O-terminated HfO_2 system (with vacancy).

O-terminated and H-passivated HfO_2 slab, one new state (band in the case of these limited supercells) is introduced within the band gap of monolayer MoS_2 (Fig. 4(a)). The conduction bands also are pulled down in comparison to the vacancy-free MoS_2-HfO_2 system in these simulations, while the valence bands show little change. The peak in AP-DOS for Hf and O atoms near 0 eV (Fig. 4(b)) correspond to the interface states arising from the missing O atom in the HfO_2 slab. These interface states would function as charge traps, leading to degradation of device performance. However, with regard to effects on the overall band structure, the O-vacancy density here is very large (areal density ≈ $1.974\times10^{14}/cm^2$) and likely exaggerates the effect.

Our simulations of monolayer MoS_2 on O-terminated Al_2O_3 with H-passivation again produce a band structure devoid of defects states, and minimal effect on the conduction bands of MoS_2 (Fig. 5(a)). With a hexagonal supercell, the Brillouin zone retains the hexagonal symmetry and the band edges for the system remain at the K point. However, unlike for the HfO_2 case, the valence bands near the Γ point are shifted up by a small amount due to mixing of O, Mo and S atom states near 0 eV, as shown in the AP-DOS plot of Fig. 5(b). In contrast to the corresponding case in the HfO_2 system, the Al-terminated Al_2O_3 slab-monolayer MoS_2 system has a limited reduction in the band gap, and interface defect states within the gap are absent (Fig. 6(a)). However, the valence band near the Γ point is lifted by a larger amount in this case than for the O-terminated Al_2O_3 slab, making the system indirect here. The greater shift can be attributed to the stronger mixing of O atoms with Mo and S atoms, as supported by the larger DOS for these

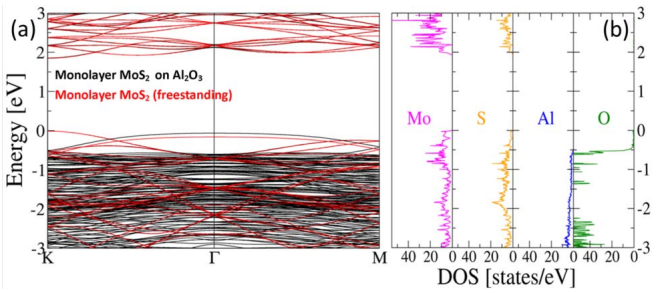

Figure 5. (a) Band structure of monolayer MoS_2 on an O-terminated Al_2O_3 slab with H-passivation, plotted along the high symmetry directions of the Brillouin zone (black lines). The band structure of freestanding monolayer MoS_2 is superimposed for comparison (red lines). (b) Atom-projected density of states for the monolayer MoS_2 and O-terminated Al_2O_3 system.

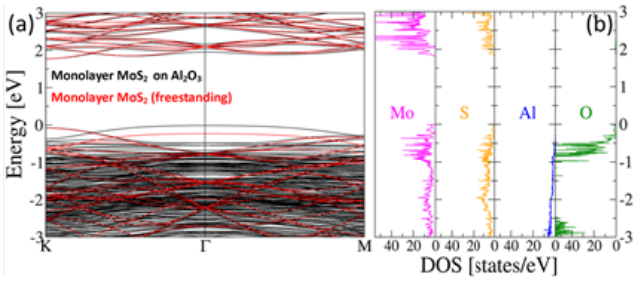

Figure 6. (a) Band structure of monolayer MoS_2 on Al-terminated Al_2O_3 slab, plotted along the high symmetry directions of the Brillouin zone (black lines). The band structure of freestanding monolayer MoS_2 is superimposed for comparison (red lines). (b) Atom projected density of states for the monolayer MoS_2 and Al-terminated Al_2O_3 system.

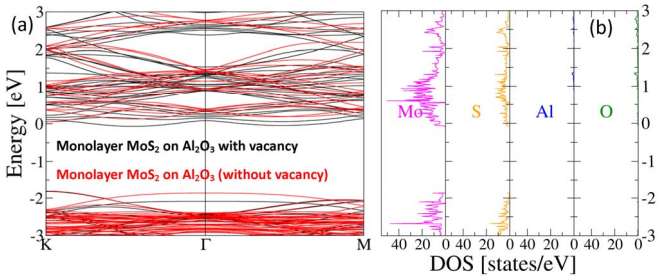

Figure 7. (a) Band structure of monolayer MoS_2 on an H-passivated, O-terminated Al_2O_3 slab with an O-vacancy in the top layer, plotted along the high symmetry directions of the Brillouin zone (black lines). The band structure of vacancy free monolayer MoS_2-Al_2O_3 system is superimposed for comparison (red lines). (b) Atom-projected density of states for the monolayer MoS_2 and O-terminated Al_2O_3 system (with vacancy).

atoms near 0 eV (Fig. 6(b)).

Creation of an O vacancy in the top O-layer of Al_2O_3 introduces new states (bands) in the immediate vicinity of the MoS_2 conduction band edge that, again, pin the Fermi level there at 0 K. These defect states, thus, perhaps would serve as effective donors. However, with again high O vacancy densities ($\approx 1.465\times10^{14}/cm^2$), the mixing of the defect states with the conduction band in these first-pass simulations is large, making precise interpretation difficult. In addition, at these high O vacancy densities, the valence band near the Γ point is pulled down, which is associated with a reduced DOS arising from the missing O atom as illustrated by the AP-DOS plot of Fig. 7(b).

IV. Conclusion

In summary, H-passivated, O-terminated HfO_2 and Al_2O_3 exhibit potential as good substrates or insulators for monolayer MoS_2, with the band structure of the composite system devoid of any interface defect states within the band gap. However, monolayer MoS_2 on Hf-terminated HfO_2 shows a significant reduction of the band gap. In comparison, Al-terminated Al_2O_3 slab looks more promising than Hf-terminated HfO_2 due to the absence of defect states. Introduction of O vacancies in the top layer of the dielectric oxide slab introduces band gap defect states in the simulated MoS_2 on O-terminated HfO_2 system, and near-conduction-band edge states that might serve as effective donors in the MoS_2 on O-terminated Al_2O_3 system.

Acknowledgment

This work is supported by SEMATECH, the Nanoelectronics Research Initiative (NRI) through the Southwest Academy of Nanoelectronics (SWAN), and Intel. We thank the Texas Advanced Computing Center (TACC) for computational support.

References

[1] Mak, Kin Fai, Changgu Lee, James Hone, Jie Shan, and Tony F. Heinz. "Atomically thin MoS_2: a new direct-gap semiconductor." *Phys. Rev. Lett.,*. vol. 105, no. 13, 2010.

[2] Radisavljevic, Branimir, Aleksandra Radenovic, Jacopo Brivio, V. Giacometti, and A. Kis. "Single-layer MoS_2 transistors." *Nat. Nanotechnol.,* vol. 6, no. 3, 2011.

[3] Chang, Jiwon, Stefano Larentis, Emanuel Tutuc, Leonard F. Register, and Sanjay K. Banerjee. "Atomistic simulation of the electronic states of adatoms in monolayer MoS_2." *App. Phy.s Lett.,*vol. 104, no. 14, 2014.

[4] Böker, Th, R. Severin, A. Müller, C. Janowitz, R. Manzke, D. Voß, P. Krüger, A. Mazur, and J. Pollmann. "Band structure of MoS_2, $MoSe_2$, and α-$MoTe_2$: Angle-resolved photoelectron spectroscopy and ab initio calculations." *Phys. Rev. B,* vol. 64, no. 23, 2001.

[5] Kang, Joongoo, E-C. Lee, and K. J. Chang. "First-principles study of the structural phase transformation of hafnia under pressure." *Phys. Rev. B*, vol. 68, no. 5, 2003.

[6] Mo, Shang-Di, and W. Y. Ching. "Electronic and optical properties of θ-Al_2O_3 and comparison to α-Al_2O_3 ." *Phys. Rev. B,* vol. 57, no. 24, 1998.